RESEARCH PAPER

The Influence of Milling Parameters on the Surface Properties in Milled AZ91C Magnesium Alloy

Amir Mostafapour[1]*, Milad Mohammadi[1], Ali Ebrahimpour[2]

* *a-mostafapur@tabrizu.ac.ir*
[1] Faculty of Mechanical Engineering, University of Tabriz, Tabriz, Iran
[2] Mianeh Technical and Engineering Faculty, University of Tabriz, Mianeh, Iran

Received: August 2020 **Revised: January 2021** **Accepted: February 2021**
DOI: 10.22068/ijmse.1971

Abstract: *A full factorial design of experiment was applied in running 36 experiments to investigate the effect of milling parameters including cutting speed, feed rate, cutting depth and machining media at two levels, on surface integration properties of magnesium AZ91C alloy such as grain size, secondary phase content, surface microhardness and roughness. In all cases, a fine grained surface with higher secondary phase sediment and micro-hardness was obtained in comparison to the raw material. According to analysis of variance results, the most effective parameter on grain size, secondary phase percent and microhardness was cutting depth and the most effective parameter on surface roughness was the feeding rate. although the grain size in all machined samples was smaller than that of the raw material but due to the dual effect of cryogenic conditions, which both cool and lubricate and reduce the temperature and strain rate at the same time, the direct effect of this parameter on grain size was not significant. The collective effect of parameters on grain size and micro- hardness was also significant.*

Keywords: *Milling, Surface roughness, Grain size, DOE, ANOVA, Magnesium alloy AZ91.*

1. INTRODUCTION

Magnesium (Mg) alloys are now becoming attractive alternate light metals for structural applications due to low density and high specific strength compared with the aluminum alloys [1]. The most popular magnesium alloys are AZ series (Mg-Al-Zn), AM series (Mg-Al-Mn), AE series (Mg-Al-RE), EZ series (Mg-RE-Zn), ZK series (Mg -Al -Zr) and series WE (Mg-RE-Zr) [2]. AZ series alloys are the most widely used group of Mg alloys in the manufacturing industry [3]. Among them, AZ91 is a die cast Mg alloy which is widely used in automobile and aerospace industries. Basically, AZ91 Mg alloy contains two phases known as α-phase which is a solid solution of Mg and Al; and β–phase (Mg 17 Al 12) which is a compound made of Mg and Al [4]. The major challenge of the Mg alloys has been their unsatisfactory corrosion resistance in a saline media [5, 6]. Previous research have shown the beneficial effects of some surface integrity (SI) parameters (such as compressive residual stress, grain refinement, strong intensity of basal texture) on the improvement of the corrosion resistance of Mg alloys [6, 7]. Therefore, the control of the corrosion rate of Mg alloys via adjusting SI, seems to be an inexpensive and effective way to produce the next generation of Mg alloys components. Several approaches have been used to improve the SI and corrosion rate of Mg alloys, such as: alloying elements, protective coatings and applying severe plastic deformation (SPD) processes [1, 3, 6, 8]. Machining is one of crucial manufacturing processes, which is widely carried out to produce structural members or components, and as a SPD process can also improve the SI. But due to the large amount of heat generated during machining, the thickness of the layer with improved SI is often very thin [9]. However, the inflammable nature; the formation of flank built up edge; higher cutting forces and surface roughness are the critical issues, which require more attention in machining of Mg alloys [10].

Lu et al. [11] reported the effect of cutting speed on the depth of affected layer thickness during turning of AZ31 Mg alloy. Poe and his colleagues [12] investigated the integrity of the surface in the drying and cryogenic machining of the alloy AZ31B with different tool radiuses . The results showed cryogenic machining using a large edge radius tool led to a thicker grain refinement layer, larger compressive residual stresses and stronger intensity of basal texture. These may remarkably enhance the corrosion performance of magnesium alloys. Wojtowicz et al [13] investigated the influence of machining conditions in turning on

[DOI: 10.22068/ijmse.1971]

surface integrity of a wrought Mg-Zn-Zr-RE. In their work, first, turned surfaces were obtained through a design of experiments, where input parameters were cutting speed, feed rate, cutting depth and nose radius. Second, modifications of surface integrity such as tensile/compressive residual stress, microhardness, twinning and surface roughness were correlated with cutting parameters. The study suggested optimal cutting conditions to achieve a given surface integrity and improve fatigue life.

In another research Oteiro and colleagues [9] studied the influence of a wide range of cutting process parameters, acting on the cutting mechanics and surface integrity produced during machining of AZ31B-O magnesium alloy. Their study has been done experimentally and numerically and the parameters were cut-ting speed, feed, tool rake angle, tool edge radius and cooling conditions. Preliminary results have shown that a minimum specific cutting energy is obtained for high values of the uncut chip thickness (or feed). This also results in an increase the compressive residual stresses as well as the thickness of the layer affected by these stresses. In other study [14] the authors considered the case of a dry plunge milling process applied to a wrought Mg-Zr-Zn-RE alloy. First, the study involved obtaining surfaces through experimental design. Second, plunge milling conditions were correlated with surface integrity factors, such as roughness, microstructure and microhardness. The study suggested plunge milling conditions to offer a trade-off between surface integrity and chip flow.

According to the literature [9], the main machining parameters are cutting speed, feed rate, cutting depth and lubrication conditions. The cutting speed has a great influence on the life of the tool, the machining forces, the surface roughness, the temperature of the machining position and the machining time. The feed rate has a direct effect on the machining efficiency but with increasing of it, the machining forces and surface roughness increases. With increasing of the cutting depth, the machining forces increase and this causes the chatter phenomenon in some cases, which in turn causes damage to the tool and workpiece. In addition, the lubrication/cooling condition has a good effect on preventing the increase of machining forces and temperature [9, 14, 15]. On the other hand, to investigate the linear and interaction effects of various process parameters on process outputs, the use of design of experiment (DOE) is a very useful method [16].

It can be seen from the previous researches that the work done in the field of AZ91 alloys machining is very limited; therefore, in this paper a comprehensive study on the effect of machining parameters on the surface integration properties of milled AZ91 parts. For this purpose, a full factorial DOE was used to create a model to calculate the influence of cutting speed (V), feed rate (F), cutting depth (D) and machining environment (C) on grain size of milled layer, surface roughness, surface microhardness and the percent of β–phase.

2. EXPERIMENTAL PROCEDURE

The mass fabrication of lightweight metal matrix castings for moderate strength applications requires the make use of high-volume die-casting techniques. The predominant magnesium alloy used for both die as well as sand casting is AZ91, containing approximately 9% aluminum and 1% zinc, which possess excellent casting properties and reasonable strength. The chemical composition of this alloy is shown in Table 1. For the preparation of specimens, casting sheets with dimensions of 140 × 60×15 mm were cut. For milling, a Sandvyk uncoated H10 grade tool with a fine-grained carbide material [17] was used. This grade has a combination of good abrasion resistance and good toughness and sharp cutting edge.

Table 1. The percentage of alloys used in the AZ91C magnesium alloy

Element	Mg	Al	Zn	Ni	Cu	Si	Fe	Mn
%	B.L	9.1	0.86	0.001	0.009	0.085	0.002	0.21

To create an orthogonal cutting condition and to avoid vibration, a triangular blade was used at an angle of 60 degrees and radius of 0.4 mm. The free angle was considered 20˚. A single-edge tool with a diameter of 20 mm was designed and manufactured according to Figure 1 (a) and (b).

All milling tests were performed by a CNC milling machine with a three-axis numerical control unit with a maximum rotational speed of 3000 rpm.

[DOI: 10.22068/ijmse.1971]

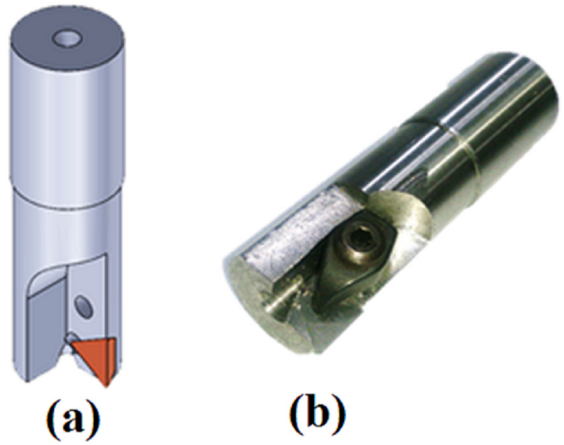

Fig. 1. (a) schematic of designed tool and (b) manufactured tool

Surface roughness measurements were carried out using a Mahr-Perthomether M2 machine with a probe radius of two microns. For each surface, two repetitions were performed on two different regions of the sample. After recording the measured values, four data were recorded for each sample and their average value was selected as the mean surface roughness number (Ra).

The average of microhardness of three different regions from a machined surface was considered as the microhardness number of that specimen. The microhardness of the surface was reported in terms of Vickers hardness and the measurements were performed under a force of 200 grams and at a time of 4 seconds.

To investigate the microstructure by optical microscope, the samples prepared by grinding and polishing and then etched in Nital 0.5% for 1 to 3 seconds. The Clemex Vision image analysis software was used to measure and compare the average size of the grains and the percentage of β-phase in OM images. The results of OM were checked by XRD pattern.

Also, field emission-scanning electron Microscopy (FE-SEM) were used for better observation of β-phase sediments and understanding their type and composition.

To study the effect of parameters, a full factorial design of experiments (DOE) was employed using Minitab 17 software. Input parameters are: cutting speed at three levels, feed rate in three levels, cutting depth in two levels and environmental conditions in two levels. According to the number of selected levels for parameters in DOE, 36 experiments were carried out and the SI parameters of surface roughness, surface hardness, grain size and β-phase sediment content were measured as the responses of the experiments. In order to increase the accuracy of the tests and to eliminate possible errors, all tests were done randomly and with tree repetitions.

For correlation of input variables and the response, a mathematical model with the ability to predict the linear, quadratic and interaction effects of the parameters on the outputs was designed according to experiments outputs. In order to minimize, maximize or achieve a certain value of response, the optimal value of the input parameters must be determined [18]. Frequently, a second-order polynomial is used as follows [18]:

$$y=\beta_0+\sum_{j=1}^{k}\beta_j x_j+\sum_{j=1}^{k}\beta_{jj}x_j^2+\sum_{i<j}\sum_{j=2}^{k}\beta_{ij}x_i x_j \quad (1)$$

where β_0 is a constant and β_{ij} is called the regression coefficient. The values, ranges and levels of the welding parameters that used in the DOE are given in Table 2. The milling parameter ranges that have been used in previous investigations [19, 20] were criteria for selection of parameters values in present study. A graphical abstract of milling process, its parameters and responses is given in Figure 2.

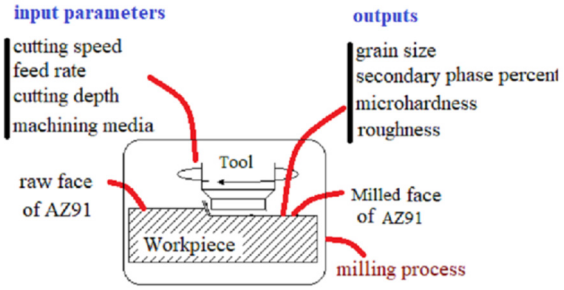

Fig. 2. A graphical abstract of milling process. Its parameters and outputs

3. RESULTS AND DISCUSSION

The microstructure images of AZ91C magnesium alloy are shown in Figures 3(a) and (b) at two different scales well. Its microstructure was characterized by the typical dendritic structure with coarse grains, as shown in Figure 3(a). This dendritic structure consisted of α–Mg matrix, Mg17Al12, β-phase precipitates, and α+β eutectic phases (Figure 3(b)). The coarse eutectic phases were distributed along the grain boundaries,

[DOI: 10.22068/ijmse.1971]

Table 2. The range of parameters and results of responses in all cases

No.	V (m/min)	F (mm/tooth)	D (mm)	C	Grain size (µm)	β-phase sediments (%)	Microhardness (Hv)	Roughness Ra (µm)
1	62.83	0.1	0.5	Dry	75.45	45.7	74.3	0.955
2	62.83	0.1	1	Dry	85.10	43.5	61.36	0.805
3	62.83	0.1	0.5	Cryogenic	75.54	38.9	72.26	0.793
4	62.83	0.1	1	Cryogenic	74.63	31.9	85.50	0.673
5	62.83	0.2	0.5	Dry	60.02	48.2	83.10	2.450
6	62.83	0.2	1	Dry	86.30	37.4	67.30	1.348
7	62.83	0.2	0.5	Cryogenic	62.41	51.2	70.40	1.911
8	62.83	0.2	1	Cryogenic	67.00	35	60.67	2.400
9	62.83	0.3	0.5	Dry	57.10	59	80.56	3.665
10	62.83	0.3	1	Dry	83.94	49.8	67.06	3.028
11	62.83	0.3	0.5	Cryogenic	75.38	48.5	73.23	3.602
12	62.83	0.3	1	Cryogenic	86.14	42.6	64.32	3.891
13	94.24	0.1	0.5	Dry	79.58	51.6	86.40	1.002
14	94.24	0.1	1	Dry	86.62	42.6	67.00	1.045
15	94.24	0.1	0.5	Cryogenic	77.52	41.4	77.20	0.81
16	94.24	0.1	1	Cryogenic	72.64	45	67.70	1.815
17	94.24	0.2	0.5	Dry	68.18	55	86.53	3.420
18	94.24	0.2	1	Dry	91.22	36.3	70.40	2.434
19	94.24	0.2	0.5	Cryogenic	67.97	55	73.37	2.714
20	94.24	0.2	1	Cryogenic	72.38	47.4	58.16	2.991
21	94.24	0.3	0.5	Dry	56.97	60	79.40	4.573
22	94.24	0.3	1	Dry	81.41	47.4	70.00	4.054
23	94.24	0.3	0.5	Cryogenic	74.42	49.6	74.23	4.259
24	94.24	0.3	1	Cryogenic	80.40	43.5	66.86	3.638
25	125.66	0.1	0.5	Dry	72.85	51.3	77.20	1.094
26	125.66	0.1	1	Dry	83.15	46	66.16	1.425
27	125.66	0.1	0.5	Cryogenic	79.97	47.5	72.26	0.42
28	125.66	0.1	1	Cryogenic	74.43	39.6	71.30	0.949
29	125.66	0.2	0.5	Dry	65.75	56.1	82.83	4.101
30	125.66	0.2	1	Dry	84.28	36.4	74.23	5.182
31	125.66	0.2	0.5	Cryogenic	68.06	59	69.53	3.374
32	125.66	0.2	1	Cryogenic	73.75	42	66.6	3.810
33	125.66	0.3	0.5	Dry	48.23	64	77.20	6.729
34	125.66	0.3	1	Dry	67.41	42.1	71.36	8.200
35	125.66	0.3	0.5	Cryogenic	70.41	55	76.20	5.662
36	125.66	0.3	1	Cryogenic	75.32	34	77.43	7.472

which were the products of a divorced eutectic reaction from the A_l enriched part of the liquid metal. A majority of the β-phase was aligned around the eutectic phases, but a few β-phase was dispersed inside α–Mg grains. The XRD pattern shown in Figure 3(c) confirmed the existence of $Mg_{17}Al_{12}$ and α-Mg phases.

Figure 3(d) and (e) illustrate the SEM image of the base metal. As can be seen, the β deposits are continuous in layers along the β-eutectic phase and dispersed in the grain boundary. The measurements carried out on the base metal show that the percentage of beta phase sediments is 29% and the average grain size is 160 microns.

All measured results for responses are given in Table 2. For developing and selecting of a model with best description of full factorial analysis, Minitab software was applied. A significant study of the model and its terms is usually done by analysis of variance (ANOVA) in factorial design method. When p-value is less than 0.05 it can be commented that the model or its terms are

[DOI: 10.22068/ijmse.1971]

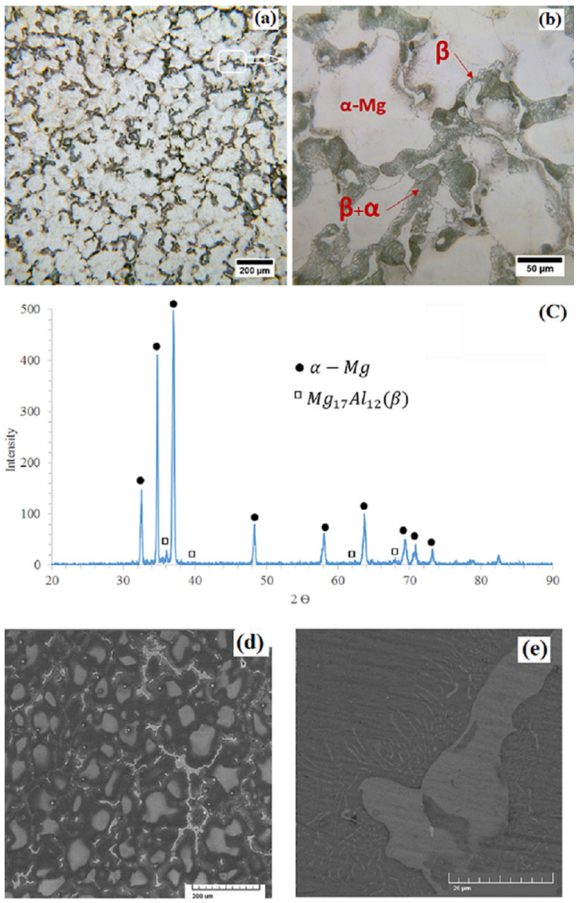

Fig. 3. (a) and (b) Optical microscopic images of AZ91C magnesium alloy at two different scales, (c) its XRD pattern and (d) and (e) SEM micrograph of base metal at two different scales

significant. Table 3 represents results of ANOVA for the responses and the influencing of input parameters on them. As said above, all of the linear and interaction effects parameters which have p-value of less than 0.05 in Table 3 are significant.

Grain size = 68.2+ 0.1282V - 92.7F + 7026C + 11.25D -0.807(V×F) + 79.2(F×C) + 127.4(F×D) - 31.2(D×C) (2)

B - Phase% = 26.1 + 0.2181V + 90.50F - 3.63C + 15.20D - 0.218(V×D) - 81.5(F×D) (3)

Microhardnes = 104.35 -0.1196V -12.65C -47.7D + 0.2415(V×D) + 10(D×C) (4)

Roughness=6.34-0.1240V-4052F+1.206C-3.11D + 0.2606(V×F) - 0.0159(V×C) + 0.062(V×D) (5)

3.1. Direct effect of input parameters

Figure 4 shows the direct influence of each parameter on responses when other parameters are constant. By increasing of cutting speed, the grain size slightly increases at first and then decreases. However, as is clear from Table 2 in all machined samples, the grain size is smaller than the base metal. The reason is that due to machining, the metal undergoes a dynamic recrystallization [20].

Machining is one of the processes in which the material undergoes severe plastic deformation and the strain rate is very high [20]. According to

Table 2. The results of ANOVA for all responses

Source	DF	Grain size		B-phase %		Microhrdness		Roughness	
		F-value	p-value	F-value	p-value	F-value	p-value	F-value	p-value
Model	19	76.10	<0.0001	13.44	<0.0001	26.20	<0.0001	52.35	<0.0001
V	2	19.94	<0.0001	6.05	0.011	17.13	<0.0001	83.93	<0.0001
F	2	72.77	<0.0001	12.65	0.001	4.10	0.037	345.17	<0.0001
D	1	459.01	<0.0001	128.29	<0.0001	256.42	<0.0001	1.38	0.258
C	1	0.34	0.567	14.46	0.002	67.78	<0.0001	5.66	0.03
V×F	4	25.81	<0.0001	2.16	0.121	4.52	0.012	23.57	0.014
V×D	2	5.85	0.012	5.97	0.012	17.56	<0.0001	10.32	0.001
V×C	2	15.13	<0.0001	1.59	0.234	4.21	0.034	5.61	0.014
F×D	2	65.95	<0.0001	10.91	0.001	4.74	0.024	0.41	0.672
F×C	2	137.25	<0.0001	1385	<0.0001	22.10	<0.0001	0	0.996
D×C	1	249.52	<0.0001	2.00	0.176	15.95	0.001	2.53	0.131
Pure error	16								
Total	35								

[DOI: 10.22068/ijmse.1971]

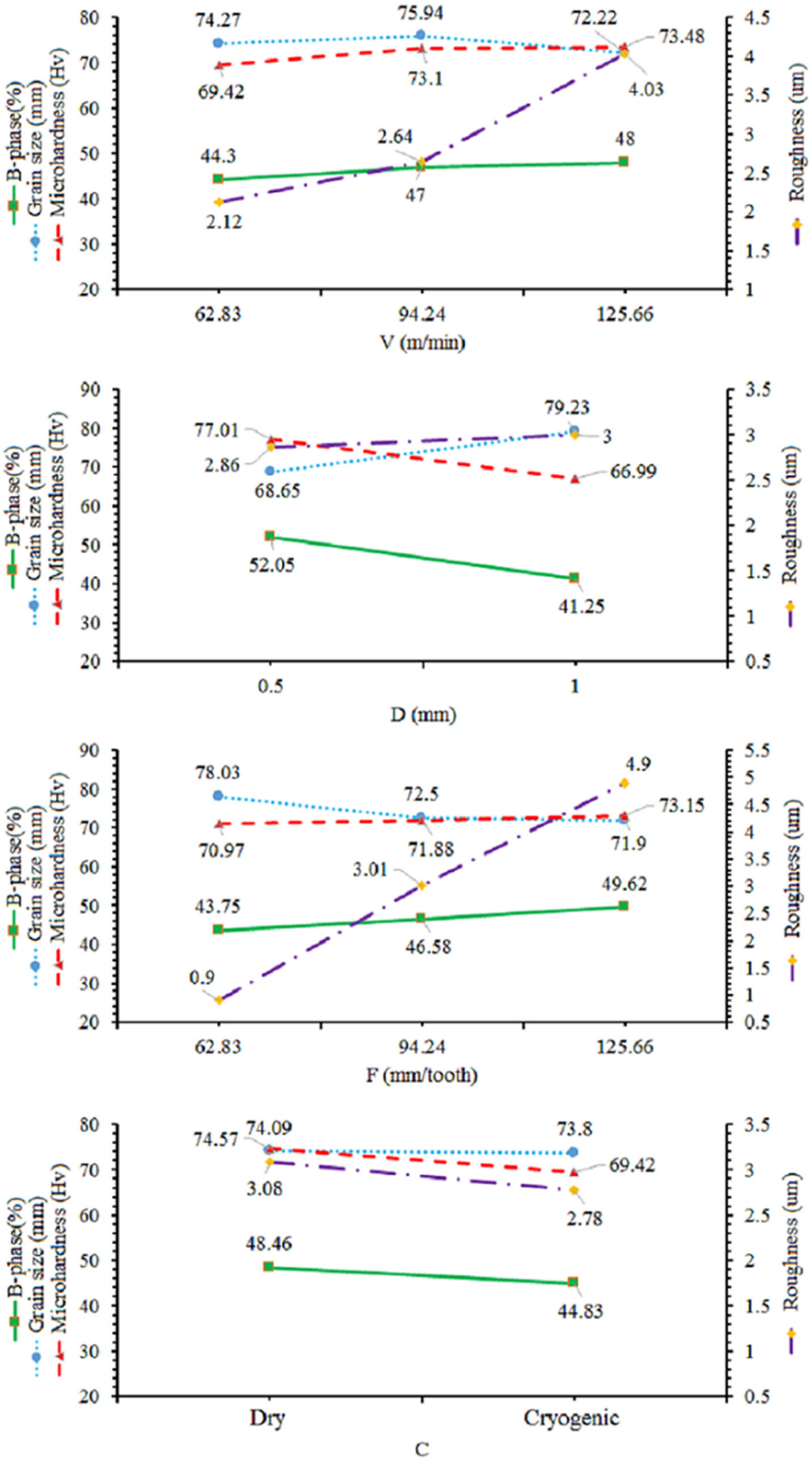

Fig. 4. The direct effects of parameters on responses

[DOI: 10.22068/ijmse.1971]

the strain rate and temperature, the Zener-Hollman parameter is defined as follows [21]:

$$Z = \dot{\varepsilon} \cdot \exp\left(\frac{Q}{RT}\right) \quad (6)$$

Where $\dot{\varepsilon}$ is the strain rate, Q is the energy of activity, R is the gas constant and T is temperature. The experimental relationship between the Zener-Hollman parameter and recrystallized grain size is as follows [21]:

$$\frac{d_{rec}}{d_{init}} = 10^3 \times Z^{-1/3} \quad (7)$$

Where d_{rec} is the size of the recrystallized grain and d_{init} is the initial grain size. Therefore, in machining due to the high strain rate, the Zener-Hollman parameter is larger and the grain size is smaller. By neglecting the slight increase in grain size at the beginning of the increasing of cutting speed (which can be related to the increase in temperature), it can be said that the grain size decreases with increasing cutting speed, due to the increase of machining forces and strain rate.

Figure 5 represents the OM microstructure of cases 6, 18 and 30, which were machined at different cutting speed (other conditions were similar) which confirms the result of Figure 4. As shown in Figures 4 and 5, increasing the cutting speed increases the amount of β-phase (dark regions in Figure 5) and, consequently, microhardness. With increasing cutting speed, plastic deformation is increased and the density of dislocations and energetic points increases for secondary phase sedimentation. In addition, surface roughness increases by cutting speed. Kim and Lee [22] reported that in a single edge tool, increasing of cutting speed causes to vibration of tool and lead to increasing of surface roughness.

From the Figure 4 (b) by increasing the feed rate from 0.1 to 0.3, the grain size decreased by an average of 8%, and the percentage of secondary phase sediments and microhardness increased by 5.9% and 3%, respectively. The microstructure of cases 1, 5 and 9 in Figure 6 confirm this claim. By increasing the feed rate the strain rate and the degree of recrystallization increases and cause to grain refinement. In fact the effect of high strain rate overcomes to effect of temperature in Zener-Holloman parameter [20]. By increasing the feed rate, due to an increase in energetic and suitable position for the formation of β-phase, the percentage of sediment and thus hardness increase. Of course, due to the increase in temperature and the tendency to dissolve sediment, the increase in sediment content and hardness is not very high. Surface roughness increases sharply by feed rate. It has been reported [13] that increasing of feed rate generates twining in the machined surface and increases the roughness.

Because of intense strain at all cutting depths, the grain size is smaller than the raw material. However, it can be seen from Figure 4 and Figure 7 that by increasing the cutting depth from 0.5 mm to 1 mm, grain size increases by about 15 percent. Because the strain rate does not increase significantly by increasing cutting depth, but the temperature reaches high level. Therefore, the grain size increases. With increasing temperature, sediments dissolves in the α-phase and the percentage of sediments reduced by about 26%. By reducing the percentage of sediments, the surface hardness decreases by about 13%.

In dry machining condition, due to the high strain rate, and dynamic recrystallization, the grain size is reduced by about 45% compared to the base metal. However, according to Table 3 the direct effect of media cooling/lubricating condition on grain size in not significant. It can be related to the dual effect of cryogenic condition which causes to cooling (temperature reduction) and lubricating (reducing of machining forces and strain rate) [20].

When using the cooling/ lubricating solution the percentage of β-phase decreases from 48.46% to 44.83 % . In addition, the hardness dropped from 74.57 up to 69.84 Hv. Layer sediments are usually formed in energetic areas such as imperfections created during high strain rate process. Decreasing β-phase causes to low microhardness in these samples [4].

3.2. Interaction effects of the parameters on responses

According to the Table 3, the all interaction effects of parameters on grain size are significant. Figure 8 shows the interaction effects of different parameters on the grain size. As can be seen, the effect of increasing the cutting depth on the increase in grain size in terms of dry machining is high (about 15%), but in a cryogenic condition, is low. Although the direct effect of the machining media on grain size was low based on ANOVA, the interactive effect of it with cutting depth

[DOI: 10.22068/ijmse.1971]

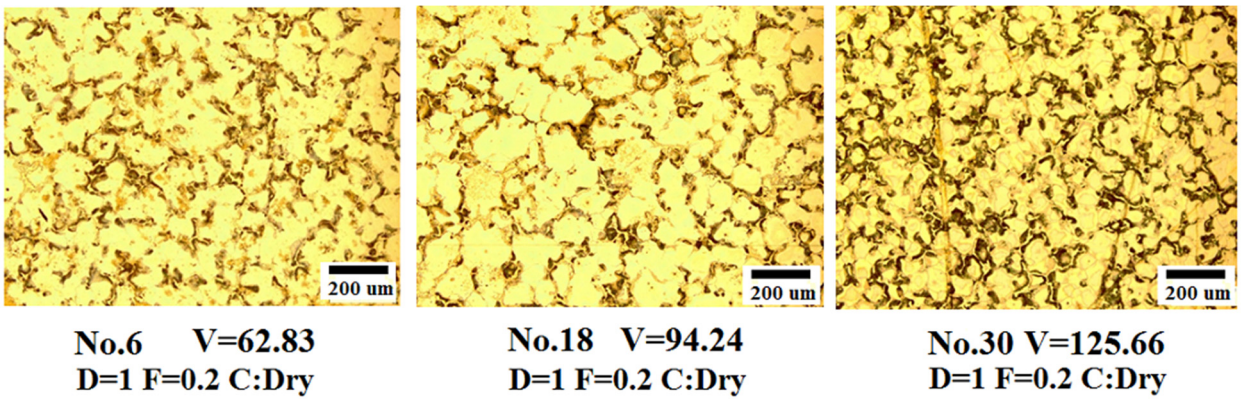

Fig. 5. Microstructure of cases number 6, 18 and 30 which were milled at various cutting speeds

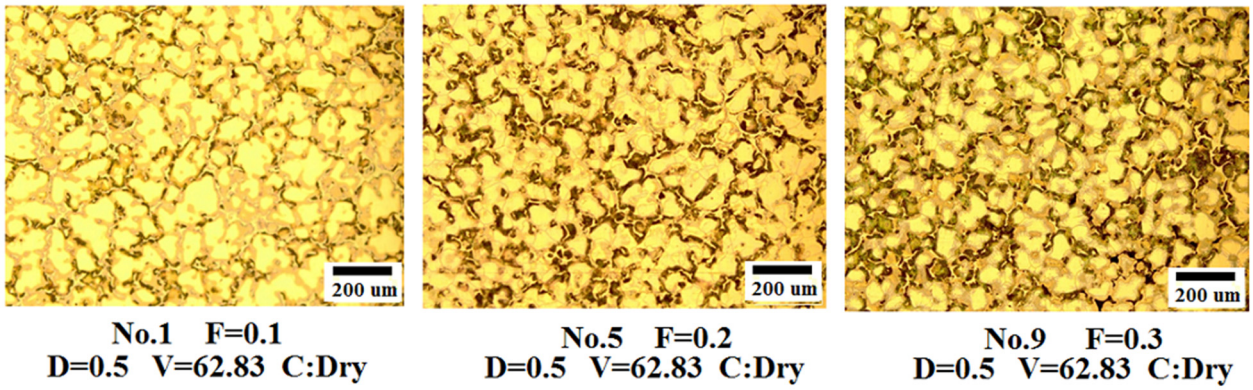

Fig. 6. Microstructure of cases number 1, 5 and 9 which were milled at various feed rates

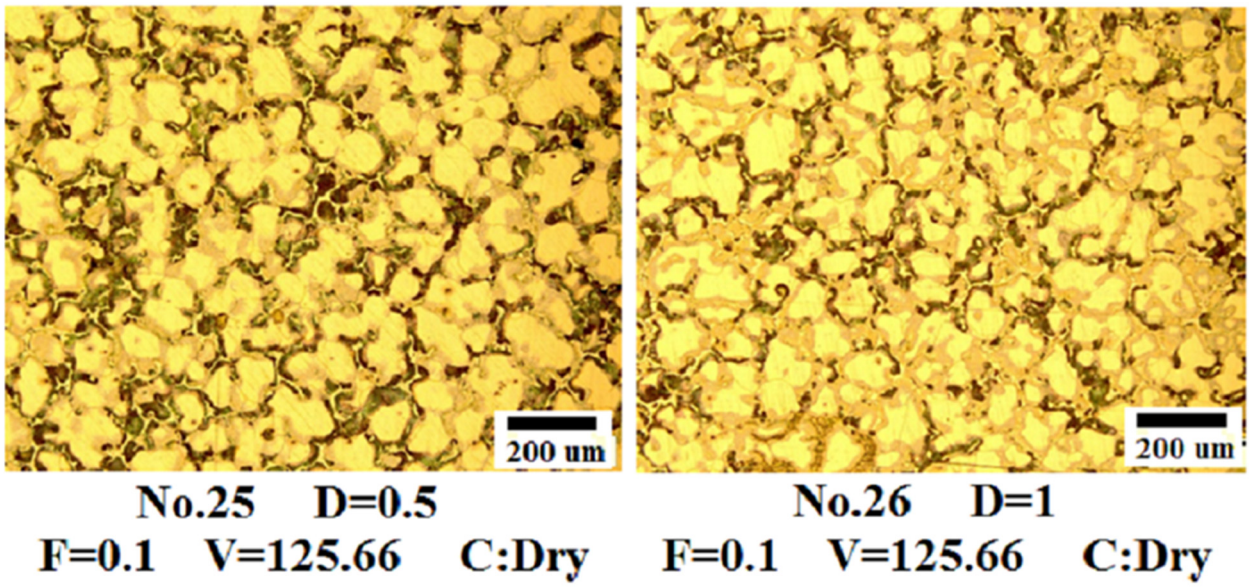

Fig. 7. Microstructure of cases number 25 and 26 which were milled at two cutting depth

[DOI: 10.22068/ijmse.1971]

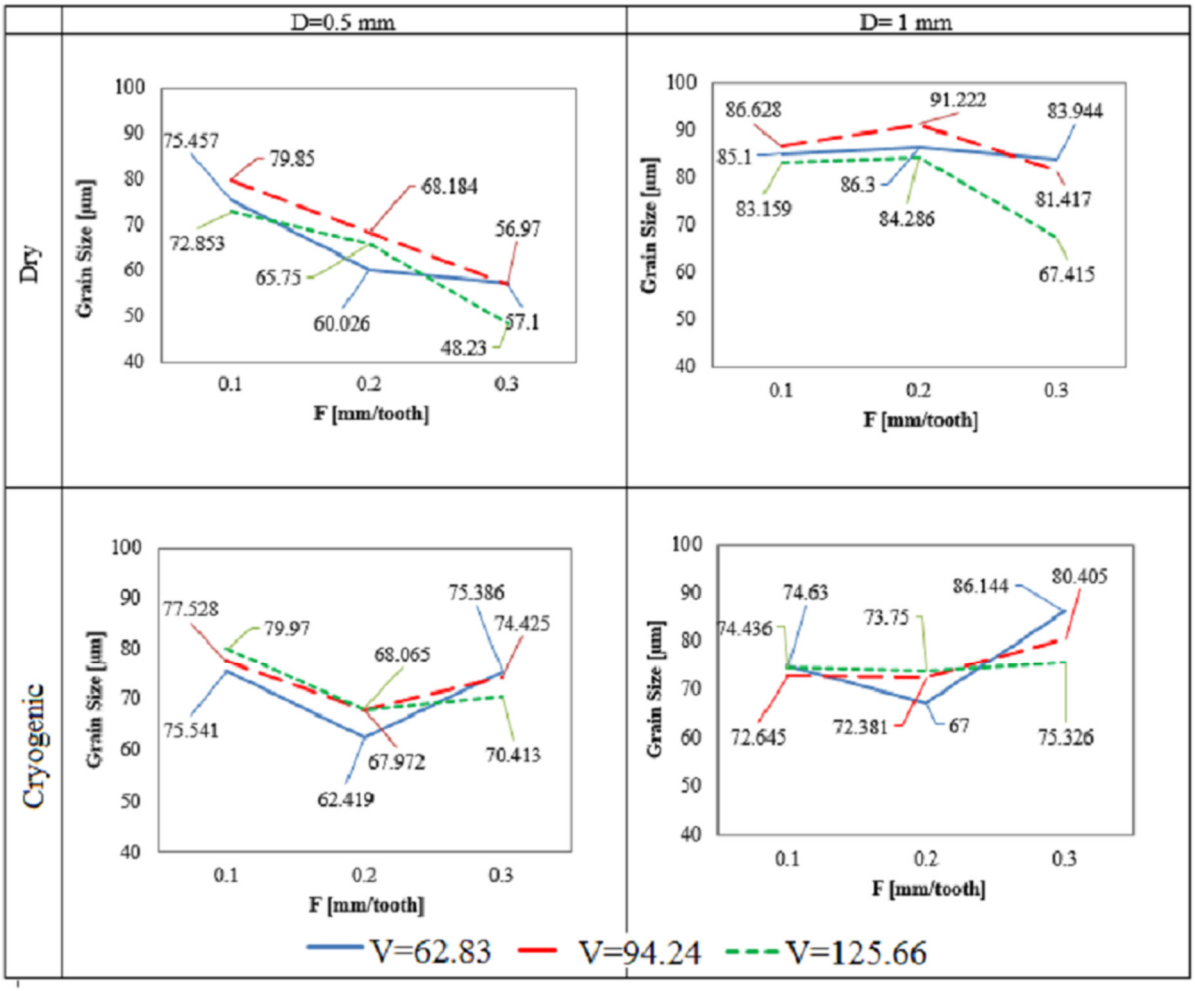

Fig. 8. Interaction effects of parameters on grain size

causes a balance in effects of temperature and strain rate and prevents changing of grain size.

At a low cutting depth and dry conditions, an increase in the feed rate leads to a reduction in the grain size, but at a higher cutting depth and the same dry condition, with increasing of feed rate, the grain size first increases slightly and then decreases. This behavior changes completely in cryogenic condition. In this case, increasing of feed rate initially decreases grain size and then increases it. These are due to the dual effect of the machining environment, which, on the one hand, causes cooling and temperature reduction, and, on the other hand, reduces the coefficient of friction and decreases the strain rate [19].

The general behavior of grain size with increasing cutting speed is such that it first increases and then decreases at high speeds. However, under low cutting depth and feed rate and cryogenic condition, increases continuously with increasing cutting speed. It also decreases continuously with increasing cutting speed at high cutting speed and feed rate and same media.

The finest grain size was obtained at a cutting depth of 0.5 mm, a feed rate of 0.3 mm/den, a cutting speed of 125.66 m/min, and a dry machining condition equal to 48.23 µm.

Based on ANOVA data in Table 3, the interaction effects V×D, F×D and F×C on β-phase percent are significant. In addition, the cutting depth has the highest direct effect and feed rate and cooling/lubrication conditions have the most important interaction effect on β-phase. Figure 9 shows the interaction effect of parameters on β-phase percent. By reducing the cutting forces and strain rate in cryogenic machining, the high energy sites for the β-phase sediments were reduced. On the other hand, increasing of feed rate caused to increasing of plastic deformation, and as a result, the density of dislocations and

[DOI: 10.22068/ijmse.1971]

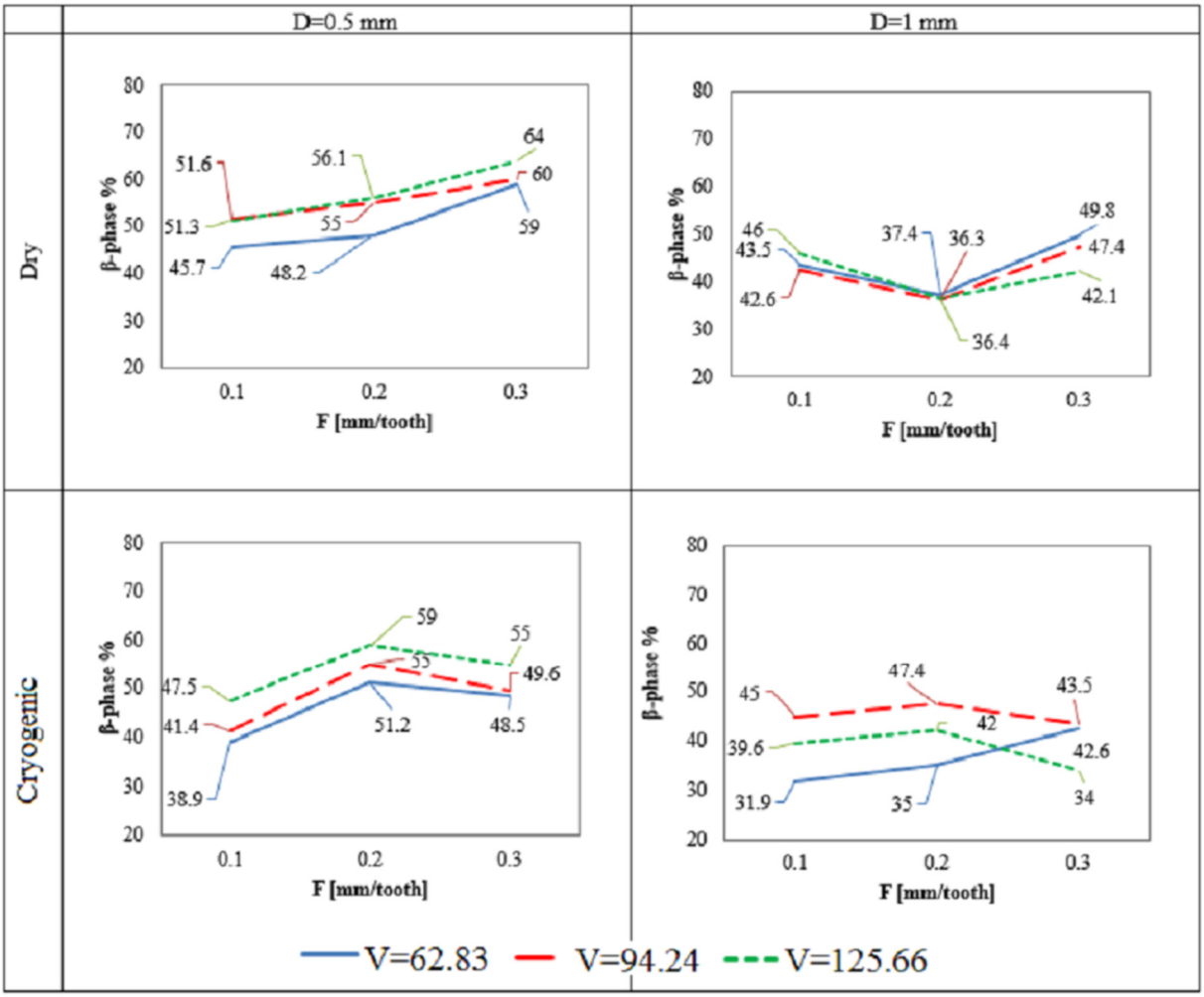

Fig. 9. Interaction effects of parameters on β-phase

high energy sites for sediments increased. Therefore, when cutting depth is low, in dry conditions, the feed rate increases the β-phase, but in the cryogenic condition, initially increases and further decreases it. However, when cutting depth is 1 mm, increasing of feed rate causes to lower β-phase sediments at first. In fact in high cutting depth, temperature rising lead to dissolution of sediments and reduction of β-phase.

The all interaction effects of parameters on mirohardness are significant according to Table 3. Since the β-phases have a higher hardness than the parent phase, it is expected that the dissolution of these sediments by increasing the temperature due to the increased cutting depth will reduce the hardness of the surface [4]. It is clear from Figure 10 that the effect of cryogenic condition on microhardness at lower cutting depth is greater (about 10%).

From ANOVA results, the interaction effects V×F, V×D and V×C on surface roughness are significant and the feed rate is most important parameter effects it. The curves that show the interaction effect of parameters on roughness are given in Figure 11. Increasing of the feed rate from 0.1 to 0.3 mm/den causes to increasing of roughness about 500%. The increase in surface roughness due to an increase in the cutting speed is approximately 85%, which is due to increased vibrations of the single edge tool [22]. It is also observed that in the cutting depth of 0.5 millimeter, the use of lubrication has a greater effect on reducing the roughness than the cutting depth of 1 millimeter. Using the lubrication at high cutting speed and the cutting depth of 1 mm has a higher effect on the surface roughness than the lower cutting depth.

[DOI: 10.22068/ijmse.1971]

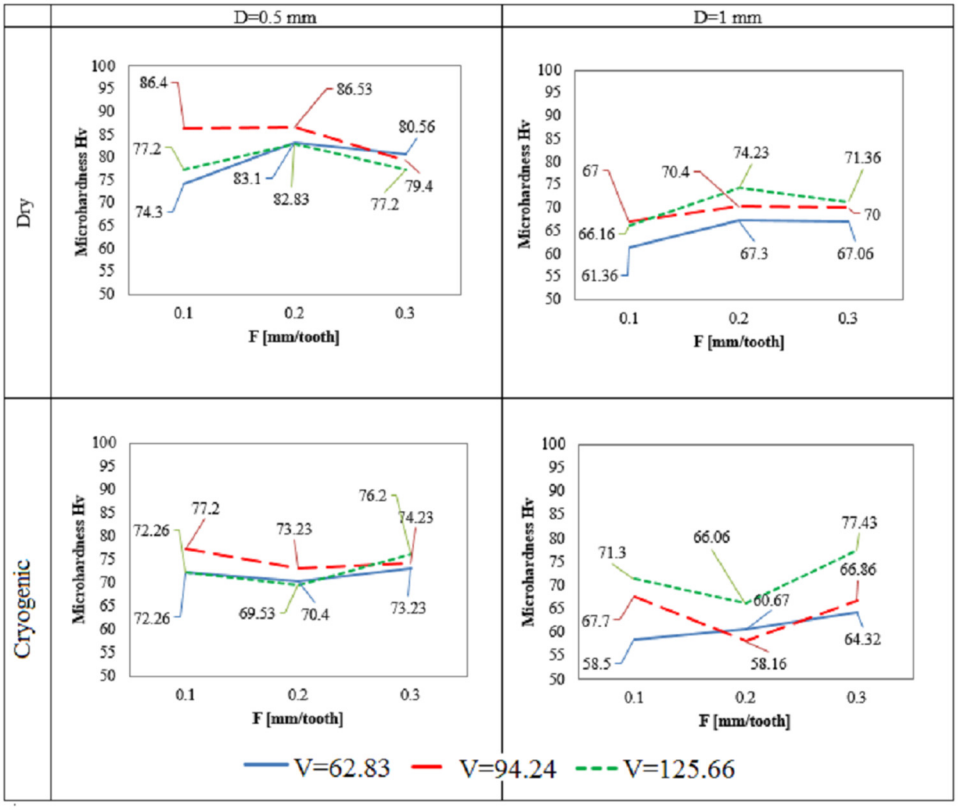

Fig. 10. Interaction effects of parameters on surface microhardness

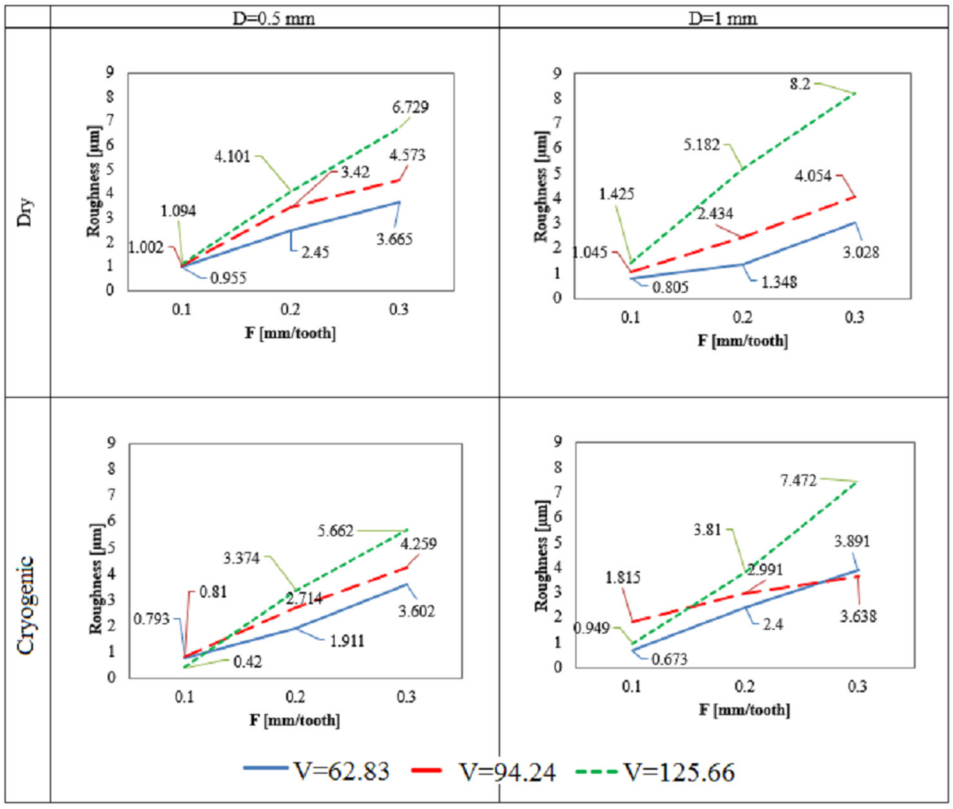

Fig. 11. Interaction effects of parameters on surface roughness

[DOI: 10.22068/ijmse.1971]

4. CONCLUSIONS

The direct and collective effect of machining parameters (cutting speed, feed rate, lubrication/cooling condition and cutting depth) on the surface integrity parameters of AZ91C magnesium alloy were investigated using a full factorial design of experiment. The following results were obtained in this study:

- The grain size decreased in all machined samples compared to the raw material.
- Increasing cutting speed from 62.83 to 125.66, led to smaller grain size. The amount of sediment increased by 8%, and consequently the hardness increased by 6%. Also, with increasing cutting speed, roughness increased by 90% due to increased vibration in the tool.
- Increasing the feed rate from 0.1 to 0.3 reduced the grain size by 8%. The percentage of secondary phase sediments and microhardness also increased by 5.9 and 3%, respectively. Also, this parameter had the greatest effect on surface roughness, which increased by about 550%.
- The grain size increased with increasing cutting depth, as the strain rate increased slightly, but the temperature increase was significant. This rise in temperature led to the dissolution of β-phase and its reduction by 26%.
- Dry machining conditions reduced the grain size in all machined samples compared to raw metal due to the proper conditions of dynamic recrystallization. But the direct effect of this parameter on grain size was not significant.
- According to ANOVA results, the collective effect of parameters on grain size and microhardness were significant. Also, the interactive effect of V×D, F×D and F×C on β-phase content and those of V×F, V×D and V×C on surface roughness were significant.

5. REFERENCES

[1] Mostafapour A., Vahedi H., Ebrahimpour A., "Experimental study on the effects of preheating time and temperature of hot press process on the mechanical and metallurgical properties of AZ91C alloy sheet."Mater. Res. Express, 2019. 6, 1-10.

[2] Bamberger M., Dehm G., "Trends in the development of new Mg alloys."Annual Review of Materials Research, 2008. 38, 505-533.

[3] Liu C., Zheng H., Gu X., Jiang B., Liang J., "Effect of severe shot peening on corrosion behavior of AZ31 and AZ91 magnesium alloys."J. Alloys Compd., 2019. 770, 500-506.

[4] Mordike B., Ebert T., "Magnesium: properties—applications—potential."Mater. Sci. Eng., A, 2001. 302, 37-45.

[5] Denkena B., Lucas A., "Biocompatible magnesium alloys as absorbable implant materials–adjusted surface and subsurface properties by machining processes."CIRP. Ann., 2007. 56, 113-116.

[6] Venkataiah M., Kumar T. A., Rao K. V., Kumar S. A., Siva I., Sunil B. R., "Effect of Grain Refinement on Corrosion Rate, Mechanical and Machining Behavior of Friction Stir Processed ZE41 Mg Alloy."Trans. Indian Inst. Met., 2019. 72, 123-132.

[7] Pu Z., Song G.-L., Yang S., Outeiro J., Dillon Jr O., Puleo D., Jawahir I., "Grain refined and basal textured surface produced by burnishing for improved corrosion performance of AZ31B Mg alloy."Corros. Sci., 2012. 57, 192-201.

[8] Guo Y., Sealy M. P., Guo C., "Significant improvement of corrosion resistance of biodegradable metallic implants processed by laser shock peening."CIRP. Ann., 2012. 61, 583-586.

[9] Outeiro J., Rossi F., Fromentin G., Poulachon G., Germain G., Batista A.,

[DOI: 10.22068/ijmse.1971]

"Process mechanics and surface integrity induced by dry and cryogenic machining of AZ31B-O magnesium alloy."Procedia CIRP, 2013. 8, 487-492.

[10] Chowdary S., Dumpala R., Kondaiah V., "Influence of heat treatment on the machinability and corrosion behavior of AZ91 Mg alloy."J. Magnes. Alloy., 2018. 6, 52-58.

[11] Lu L., Hu S., Liu L., Yin Z., "High speed cutting of AZ31 magnesium alloy."J. Magnes. Alloy., 2016. 4, 128-134.

[12] Pu Z., Outeiro J., Batista A., Dillon O., Puleo D., Jawahir I., "Surface integrity in dry and cryogenic machining of AZ31B Mg alloy with varying cutting edge radius tools."Procedia. Eng., 2011. 19, 282-287.

[13] Wojtowicz N., Danis I., Monies F., Lamesle P., Chieragati R., "The influence of cutting conditions on surface integrity of a wrought magnesium alloy."Procedia. Eng., 2013. 63, 20-28.

[14] Danis I., Wojtowicz N., Monies F., Lamesle P., Lagarrigue P., "Cutting conditions and surface integrity during dry plunge-milling of a wrought magnesium alloy."Procedia. Eng., 2013. 63, 36-44.

[15] Viswanathan R., Ramesh S., Subburam V., "Measurement and optimization of performance characteristics in turning of Mg alloy under dry and MQL conditions."Measurement, 2018. 120, 107-113.

[16] Mostafapour A., Ebrahimpour A., Saeid T., "Finite element investigation on the effect of FSSW parameters on the size of welding subdivided zones in TRIP steels."Int. J. Adv. Manuf. Technol., 2017. 88, 277-289.

[17] "Rptating tools catalogue", www.sandvik.coromant.com

[18] Khuri A. I., Mukhopadhyay S., "Response surface methodology. "Wiley Interdisciplinary Reviews: Computational Statistics, 2010. 2, 128-149.

[19] Pu Z., Outeiro J., Batista A., Dillon Jr O., Puleo D., Jawahir I., "Enhanced surface integrity of AZ31B Mg alloy by cryogenic machining towards improved functional performance of machined components."Int. J. Mach. Tools Manuf., 2012. 56, 17-27.

[20] Pu Z., "Cryogenic machining and burnishing of AZ31B magnesium alloy for enhanced surface integrity and functional performance", 2012. Ph D Thesis, University of Kentucky.

[21] Chang C., Du X., Huang J., "Achieving ultrafine grain size in Mg–Al–Zn alloy by friction stir processing."Scripta Mater., 2007. 57, 209-212.

[22] Kim J.-D., Lee K.-B., "Surface roughness evaluation in dry-cutting of magnesium alloy by air pressure coolant."Engr., 2010. 2, 788-793.

[DOI: 10.22068/ijmse.1971]